Quadrupole Induced Resonant Particle Transport in a Pure Electron Plasma

E. P. Gilson* and J. Fajans†

*Plasma Physics Laboratory, Princeton University, Princeton, New Jersey, 08543
†Department of Physics, University of California, Berkeley, California, 94720

Abstract. We performed experiments that explore the effects of a quadrupole magnetic field on a pure electron plasma confined in a Malmberg-Penning trap. This work is important both as an example of resonant particle transport and for antihydrogen ($\bar{H}$). The $\bar{H}$ experiments plan to use magnetic quadrupole neutral atom traps to confine $\bar{H}$ atoms created in double-well positron/antiproton Malmberg-Penning traps. Our results show that a quadrupole field of only 0.020 G/cm can cause significant transport when applied to a 1 cm radius plasma confined by an axial field of 100 G. Our model describes the shape of the plasma and shows that resonant electrons follow trajectories that take them on large radial excursions, leading to enhanced transport. If the electrons are off resonance, then diffusion will not be greatly enhanced. The measured diffusion scales like the square of the quadrupole field strength, inversely like the square of the axial magnetic field and, below resonance, like the square of the $\boldsymbol{E} \times \boldsymbol{B}$ rotation frequency. The location of the resonance in parameter space scales accordingly as we vary the length and temperature of the plasma. However, the temperature used in fitting the data differs from the independently measured temperature by a factor of four, suggesting that our description of the effect as purely diffusive is not correct.

INTRODUCTION

Antihydrogen ($\bar{H}$) experiments at CERN by the ATHENA [1] and ATRAP [2] collaborations need to trap antihydrogen, antiprotons and electrons in the same place. However, neutral atom traps with magnetic field gradients may not be compatible with Malmberg-Penning traps because magnetic field gradients break the cylindrical symmetry of Malmberg-Penning traps, degrading their confinement properties. This asymmetry induced transport may prevent the use of Malmberg-Penning traps in $\bar{H}$ experiments. Beyond its immediate importance to $\bar{H}$ research, this phenomenon is also of interest in the general plasma community. It is relevant both in the study of resonant particle transport in Malmberg-Penning traps [3, 4, 5, 6, 7, 8] and in tandem mirror machines [9, 10, 11, 12, 13].

We have applied an axially invariant, transverse, quadrupole magnetic field to a pure electron plasma confined in a Malmberg-Penning trap and observed its effects on the shape of the plasma and on transport. We find that the shape of the plasma follows the surface of a magnetic flux tube if the bulk rotation of the plasma is slow compared to the axial bounce time of the electrons. The plasma shape is cylindrical if the bulk rotation of the plasma is fast compared to the axial bounce time. Measurements of the radial transport show a strong resonant behavior that is not in complete agreement with our model of the effect, but is consistent with many of the predicted scalings. We expect that

this transport will make it difficult to confine antiprotons and positrons long enough to create $\bar{H}$ atoms.

EXPERIMENT

We apply a transverse, axially invariant, quadrupole magnetic field to a Malmberg-Penning trap using two different sets of coils. We can apply a transverse quadrupole field at any angle, θ_o by adjusting the relative current in each coil. The total magnetic field is then

$$\boldsymbol{B} = B_z\hat{\boldsymbol{z}} + \beta_1\left(x\hat{\boldsymbol{x}} - y\hat{\boldsymbol{y}}\right) + \beta_2\left(y\hat{\boldsymbol{x}} + x\hat{\boldsymbol{y}}\right), \tag{1}$$

where $\beta = \sqrt{\beta_1^2 + \beta_2^2}$ is the strength of the quadrupole field in G/cm and $\tan(2\theta_0) = \beta_1/\beta_2$. In our experiment, the axial field ranges from $40 - 1500$ G, while $\beta \leq 1.0$ G/cm for the coils we constructed. Even though these quadrupole fields are weak compared to B_z at a typical plasma radius of 1 cm, we find that they produce strong transport. Figure 1 shows that a flux tube that is circular at $z = 0$ is elliptical at either end, but with the ellipses rotated by 90° with respect to one another.

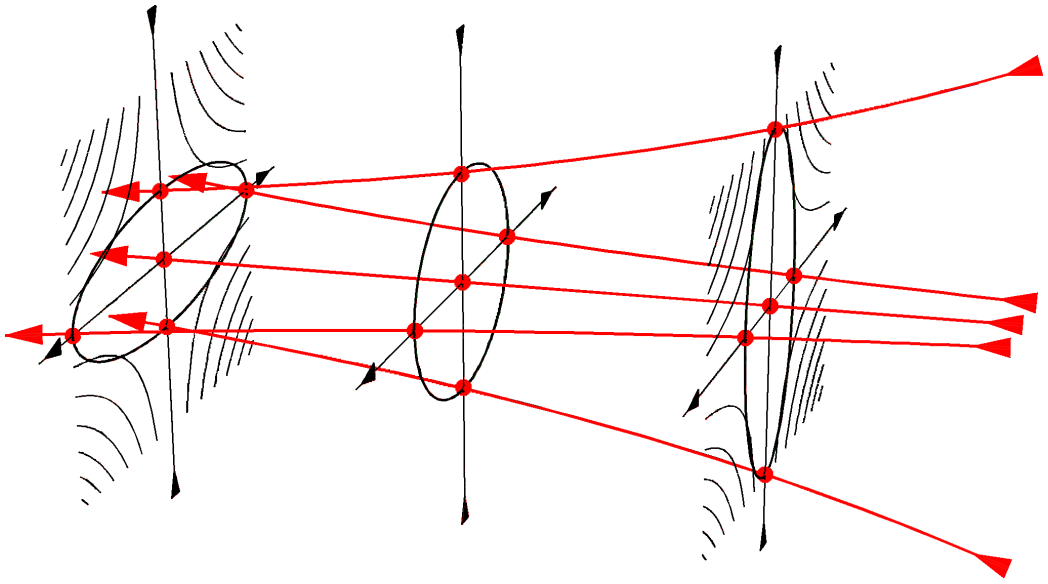

FIGURE 1. The lines with arrows show the field lines produced by adding a small, transverse, quadrupole field with $\theta_o = 0$ to a strong axial field. A flux tube that is circular at $z = 0$ is elliptical as you move away from $z = 0$. The transverse cross sections show the field lines for the transverse quadrupole field alone.

The quadrupole field has four-fold symmetry and so there exists a resonance condition,

$$\omega t_b = \frac{N\pi}{2}, \tag{2}$$

for which an electron rotates about the trap axis by $N\pi/2$ radians as it travels across the length of the trap. The rotation frequency about the trap axis is given by the $\boldsymbol{E}\times\boldsymbol{B}$ frequency, ω, and the bounce time is given by $t_b = L/v_z$. We show below that the $N = 1$

resonance is the most important resonance and so we say that if $\omega t_b \gg \pi/2$, the electron is above resonance and if $\omega t_b \ll \pi/2$, the electron is below resonance.

We measure the effects of the quadrupole field using both the wall of the trap and a phosphor coated glass substrate. We use the trap wall to detect the image charge on a confinement gate that is divided into four azimuthal sectors of 90° extent. This allows us to measure the quadrupole moment of the plasma at the axial location of the gate. The phosphor collects the dumped plasma, producing an image whose brightness is proportional to the z-integrated plasma density, $n(r,\theta)$. We extract radial transport quantities from these plasma images.

PLASMA SHAPE

The quadrupole field changes the trajectories of the electrons and thus changes the shape of the plasma. With transport present, the plasma's density and shape change with time. If the characteristic transport time is greater than the other time scales in the system, then we can imagine that the plasma exists in a quasi-equilibrium state at any instant in time. It is the shape of the quasi-equilibrium plasma that we are interested in.

Measures of the plasma's shape are the ellipticity, ε, and the orientation angle, θ_p. The ellipticity is the RMS length of the plasma cross section divided by the RMS width, and θ_p is the angle that the major axis of the ellipse makes with the x axis. We can measure ε and θ_p either directly from the plasma images or from the signal induced on the wall of the trap as measured by the four-sectored gate. The signal that we use to measure the quadrupole moment is the combination $(V_1+V_3)-(V_2+V_4) \propto \varepsilon - 1$, where V_i are the voltages induced on the wall sectors.

We expect that when $\overline{\omega t_b} \ll 1$ (where the overbar denotes some suitable average value for the plasma as a whole), the electrons largely follow the field lines in Figure 1. The plasma has the shape of a magnetic flux tube. We expect that when $\overline{\omega t_b} \gg 1$, the radial oscillations average out and the plasma is cylindrical. The data in Figure 2, derived from plasma images, show that the plasma changes from elliptical at small $\overline{\omega t_b}$ (large B_z) to cylindrical at large $\overline{\omega t_b}$ (small B_z). At large B_z, $\theta_p \approx \theta_o = -45°$ and gradually changes to $\theta_o + 90°$ at small B_z. This rotation away from θ_o at low B_z is likely due to the effects of the radial component of the imaging field we use. At lower B_z, the imaging field creates a larger $\boldsymbol{E} \times \boldsymbol{B}$ rotation. Lastly, we see that by scaling out a factor of β, the data for various β/B_z coincide. Thus, $\varepsilon - 1$ at a given B_z is proportional to β.

Using the wall sectors, we explore the z dependence of the below-resonance ($\overline{\omega t_b} \ll 1$) plasma shape. We measure ε at the end of several plasmas with different lengths at fixed β and we find that $\varepsilon - 1$ at the end of the plasma is proportional to L. We measure ε at the middle, left end, and right end of a plasma and the data in Figure 3 demonstrate that $\varepsilon - 1$ is equal and opposite at $\pm z_o$ and is 0 at $z = 0$. Further, $\varepsilon - 1$ is also proportional to β. Unfortunately, it is not possible to verify the axial invariance of the above-resonance ($\overline{\omega t_b} \gg 1$) plasma in our experiment because we cannot simultaneously move the four-sectored gate around and be in the above-resonance regime.

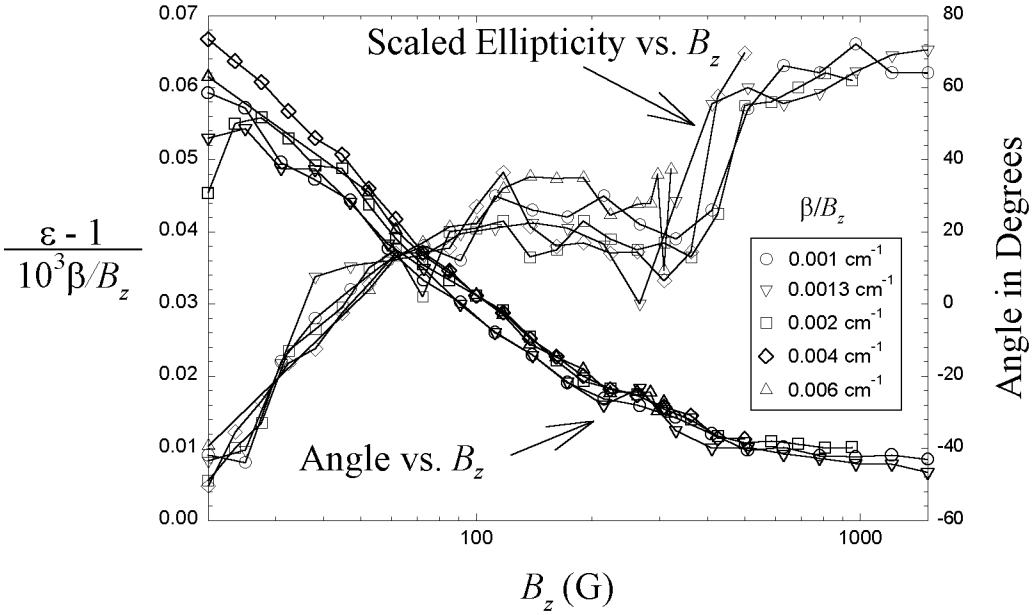

FIGURE 2. Varying B_z changes ω and thus $\overline{\omega t_b}$. $\varepsilon(B_z) - 1$ approaches zero at low B_z (large ωt_b) and is proportional to β. $\theta_p \approx \theta_o = -45°$ at large B_z and the change in $\theta_p(B_z)$ is likely due to imaging fields.

TRANSPORT

We envision the effect of the quadrupole field to be a diffusion process. The quadrupole field causes electrons to have trajectories with radial excursions. The smallest collisions, however, can knock electrons from one trajectory to another. We study transport using a simplified model in which we can find the electron trajectories analytically. We estimate the step size, λ, from these trajectories, postulate a collision frequency, ν, and form a diffusion coefficient, $D = \lambda^2 \nu f$, where f is the fraction of electrons participating in the diffusion.

We can guess what the trajectories look like by considering several examples. Figure 4 shows that a resonant electron ($\omega t_b = \pi/2$) that starts at 45° below the x axis is on field lines with radial components directed radially outwards as it bounces back and forth across the trap. This resonant electron moves to a larger radial position than it started at. For $N > 1$, N odd, there are the higher order resonances with smaller radial excursions. For N even, the radial displacements cancel. For other initial angles and other values of ωt_b, the trajectories may move inwards or oscillate radially.

If the guiding center of an electron follows a magnetic field line, then

$$\frac{dr}{dt} = \frac{\beta r v_z \cos[2\theta(t)]}{B_z}. \tag{3}$$

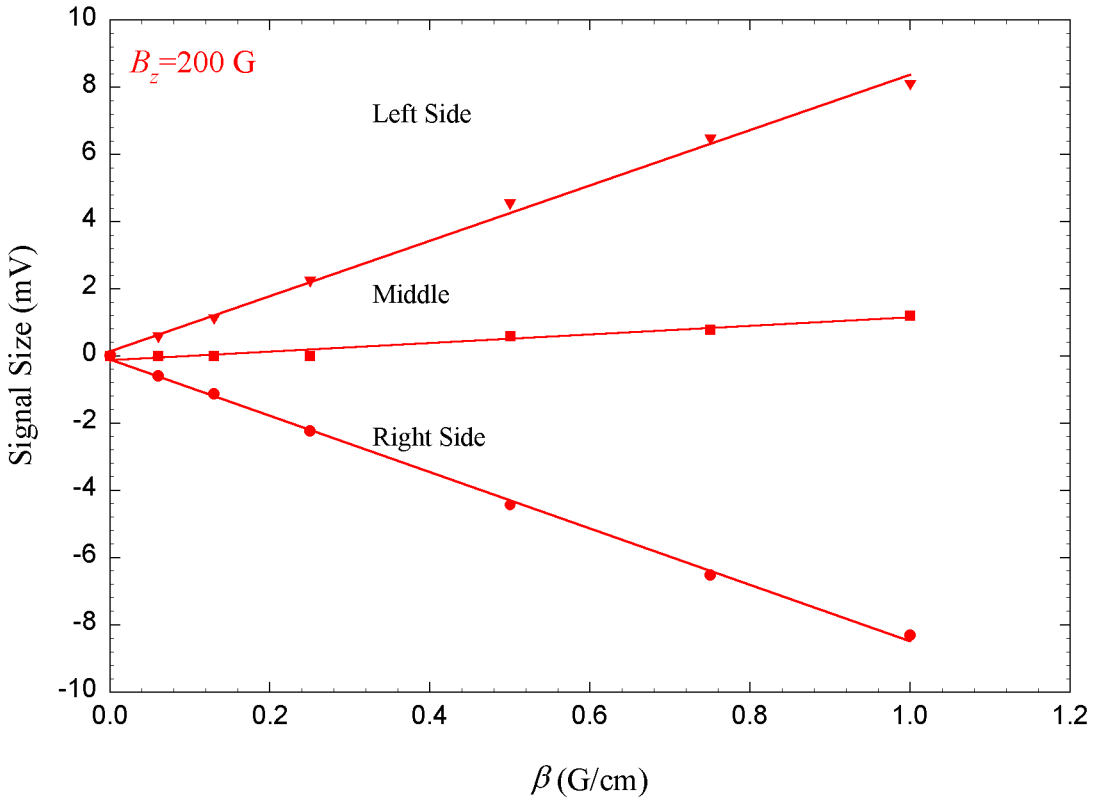

FIGURE 3. Placing the pickup gate at different axial positions ($z = 0, \pm 10.3$ cm) allows us to measure the relative ellipticity at the left, middle, and right of the plasma. We see that the signal in the center of the plasma vanishes, while the signal is equal and opposite at the ends of the plasma. The signal is proportional to β.

Because frequent collisions will disturb the electrons before they can go very far, we estimate the step size to be $\lambda = r(\nu^{-1}) - r_o$.

$$\lambda \approx r_o \left(\frac{4\omega L \beta}{B_z N^2 \pi^2 \nu} \right), \tag{4}$$

where we have assumed that $\theta(t) = \omega t - \pi/4$ and that we can replace v_z with $2\omega L/N\pi$ by virtue of the resonance condition in Eq. (2).

Since electrons that are not exactly resonant also contribute to the transport, we must calculate the width of the resonance. For a given v_z, there is a resonant rotation frequency ω_R and we define the width of the resonance, $\Delta\omega$, through the relationship, $\omega = \omega_R + \Delta\omega$. To determine $\Delta\omega$, we note that the solution of Eq. (3) depends on $\Delta\omega$ through its dependence on $\theta(t) = \omega t + \theta_o = (\omega_R + \Delta\omega)t + \theta_o$. Since the solution to Eq. (3) is an oscillatory function, we choose $\Delta\omega$ so that $t = \nu^{-1}$ corresponds to the first maximum of $r(t)$. This is equivalent to requiring that the extra angle of rotation, $\Delta\phi = \Delta\omega/\nu$, before a collision should be no greater than $\pi/4$.

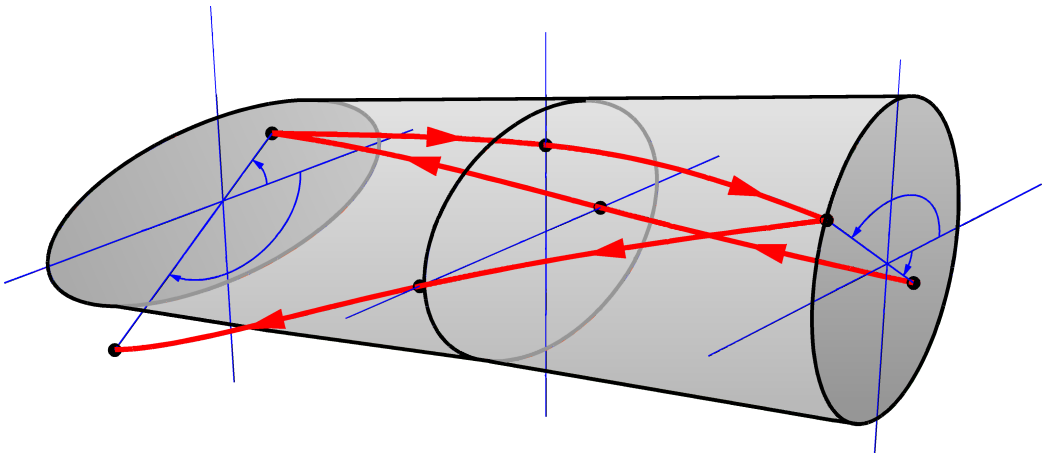

FIGURE 4. An electron that begins 45° below the x axis and rotates by 90° as it travels the length of the trap is resonant and moves ever outwards.

We construct the diffusion coefficient by writing $f = \sqrt{m/2\pi kT}\exp(-v_z^2/2v_{th}^2)\Delta v_z$, where $v_{th} = \sqrt{kT/m}$. Since the resonant electron has $\omega = (N\pi/2)(v_z/L)$, we can write $\Delta\omega/\omega = \Delta v_z/v_z$, or $\Delta v_z = L\nu/2N$. Putting this all together gives

$$D_N = r_o^2 \frac{8\omega^2 L^3 \beta^2}{B_z^2 N^5 \pi^4} \sqrt{\frac{m}{2\pi kT}} \exp\left(-\frac{\omega^2}{2\omega_{th}^2}\right), \tag{5}$$

where $\omega_{th} \equiv N\pi v_{th}/2L$. Summing over odd N gives the total diffusion. However, the factor of N^{-5} implies that the diffusion is dominated by the $N = 1$ resonance.

We may describe the resonant behavior of $D_N(\omega)$ qualitatively. Above resonance, the plasma is rotating relatively quickly, and so for an electron to be resonant it must have a relatively large v_z. But the Maxwellian distribution ensures that there are few electrons moving very fast and so the diffusion is suppressed. Below resonance, there are plenty of resonant electrons in the thermal distribution, but now the step size is small and again, diffusion is suppressed.

The scaling of D with β^2 and the cancellation of the collision frequency, ν, are typical of diffusion in the so-called "plateau" regime. $D_N(\omega)$ has a maximum, D_{max}, at $\omega_{res} = \sqrt{2}\omega_{th}$. Therefore, D_{max} scales like $\omega^2\exp(-\omega^2/2\omega_{th}^2)|_{\omega_{res}} \approx \omega_{th}^2$. This makes the overall L scaling of D_{max} $L^3\omega_{th}^2 \propto L$, and the overall kT scaling $\omega_{th}^2/\sqrt{kT} \propto \sqrt{kT}$.

When $\omega \ll \omega_{th}$ (below resonance), the exponential term is close to unity and can be ignored. In this regime, $D \propto (\beta r_o \omega/B_z)^2 L^3$. Since $\omega \propto 1/B_z$, D scales like L^3/B_z^4, in contrast to the usual L^2/B_z^2 that is attributed to resonant particle transport [4]. But, if β/B_z is constant, as would be the case if the quadrupole field perturbation came from asymmetries in the solenoidal magnet, the scaling is L^3/B_z^2.

To measure D from $n(r,t)$, we manipulate the diffusion equation to give,

$$D = \frac{dN/dt}{2\pi r_o\, dn/dr|_{r=r_o}}, \tag{6}$$

where $N(t) = \int_0^{r_o} n(r,t)\, 2\pi r\, dr$. We measure the slope dn/dr from a single image with $n(r) = \frac{1}{2\pi}\int_0^{2\pi} n(r,\theta)\, d\theta$. The θ-averaging is acceptable because the quadrupole fields used for transport measurements are small enough that the plasma shape is cylindrical, even for the below-resonance plasmas. We image plasmas held for different times to measure the time dependence of $n(r,t)$. We choose a radius, r_o, calculate $N(t)$ and compute dN/dt. The choice of t is arbitrary since we do not expect transport to have an explicit time dependence and we choose t by some auxiliary condition, for example to have $\omega(r_o)$ be constant across a data set.

We measure $D(\beta_1, \beta_2)$ for many ω, B_z, L, and kT. Figure 5 shows a typical plot of D versus the transverse quadrupole field. We find that the minimum diffusion does not occur at zero perturbation. This is evidence that we are correcting for naturally occurring field errors by applying a quadrupole field. The surfaces $D(\beta_1, \beta_2)$ allow us to verify the β^2 scaling predicted by the model. We find that, over parameters available to us ranging from $\omega = 8.0 \times 10^5$ rad s^{-1} to 3.0×10^6 rad s^{-1}, D scales like β^2.

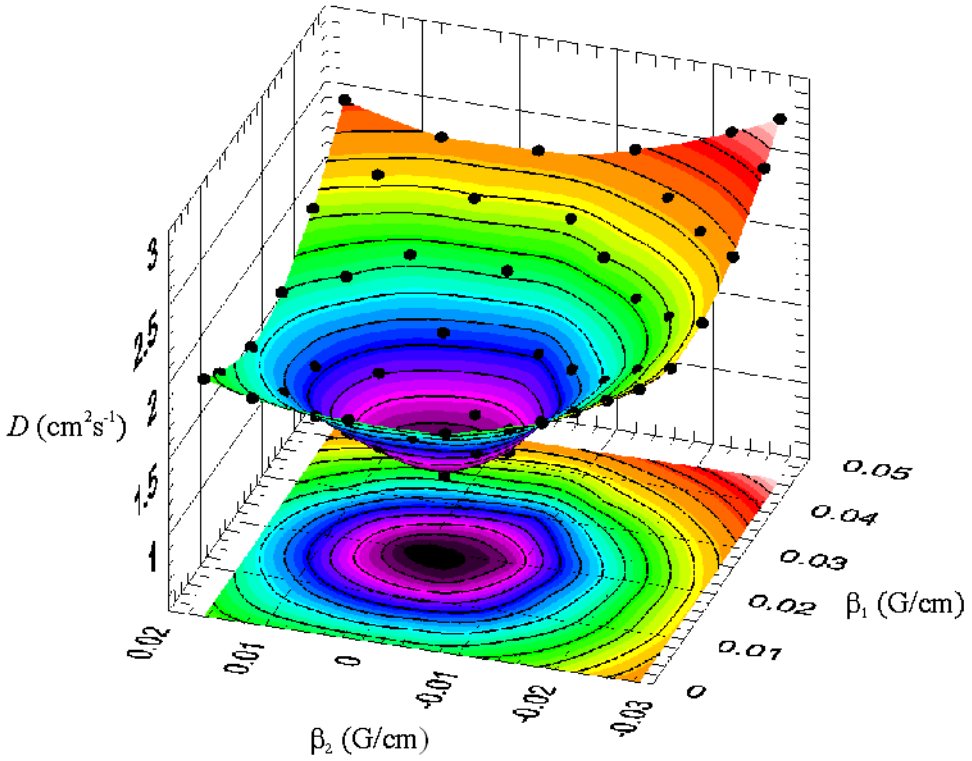

FIGURE 5. Diffusion from the application of a quadrupole field. This data is taken at $B_z = 100$ G, $r_o = 0.95$ cm, and $\omega = 2.0 \times 10^6$ rad s^{-1}. We choose values of β_1 and β_2 in a checkerboard pattern and the data (solid dots) show that there is an optimal quadrupole field and that diffusion increases away from this optimal value.

We investigate the ω dependence of the phenomenon by measuring the average D at a distance of $\beta = 0.020$ G/cm from the minimum of the $D(\beta_1, \beta_2)$ surface. This averaging over θ_o dominates statistical uncertainty in D of approximately 7%. Figure 6 shows $DB_z^2(\omega)$ for several B_z, $L = 28$ cm, $r_o = 0.95$ cm, and $kT = 1.6$ eV. The data show that the quadrupole field enhances diffusion resonantly in ω. As ω increases from 10^5 rad s^{-1},

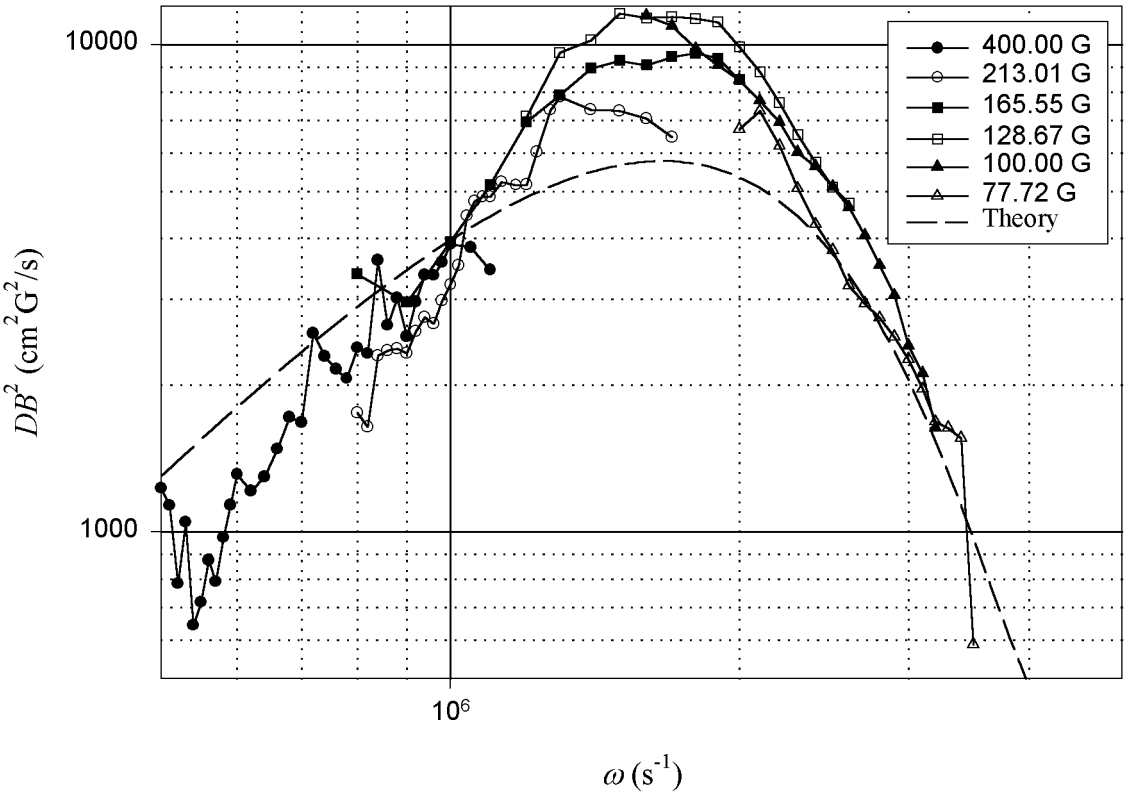

FIGURE 6. DB_z^2 shows a strong resonance in ω. There is an explicit B_z^{-2} dependence and for small ω the diffusion scales like ω^2. The theory fit agrees best with the data if we use a multiplicative factor of 0.3 and an artificially low temperature of 0.34 eV. The independently measured temperature is 1.6 eV.

the diffusion grows. But above $\omega \approx 2 \times 10^6$ rad s^{-1} the diffusion decreases again. We observe that there is an explicit B_z^{-2} scaling, since the data for various B_z in Figure 6 overlap. Our formula for D scales like ω^2 at small ω and a least squares fit to the data with $\omega < 1.3 \times 10^6$ rad s^{-1} gives an exponent of 2.05 ± 0.09.

To be a bounce resonant effect, the peak in ω should shift as we vary L and kT. We repeat the measurements of D as a function of ω as in Figure 6 for plasmas with smaller L. Figure 7 shows that the peak moves to larger ω as L decreases, although the exact dependence on L is difficult to obtain from these data. We find that $D_{\max}$ decreases as L decreases. To test the temperature dependence, we heated the plasma for 1 ms by applying a noise signal to the wall of the trap after injecting the plasma. Although the resonance moves to larger ω, we observe that $D_{\max}$ decreases as kT increases. Our model predicts that $D_{\max}$ should increase as kT increases.

Figure 6 includes a curve representing our model with terms up to $N = 10$. The theory curve shows moderate agreement with the data if we use an overall multiplicative factor of about 0.3, and set kT to be 0.34 eV. A multiplicative factor of order unity might be expected given the rough nature of our calculation. However, independent measurements of kT give $kT = 1.6$ eV and this discrepancy is more serious and remains unexplained.

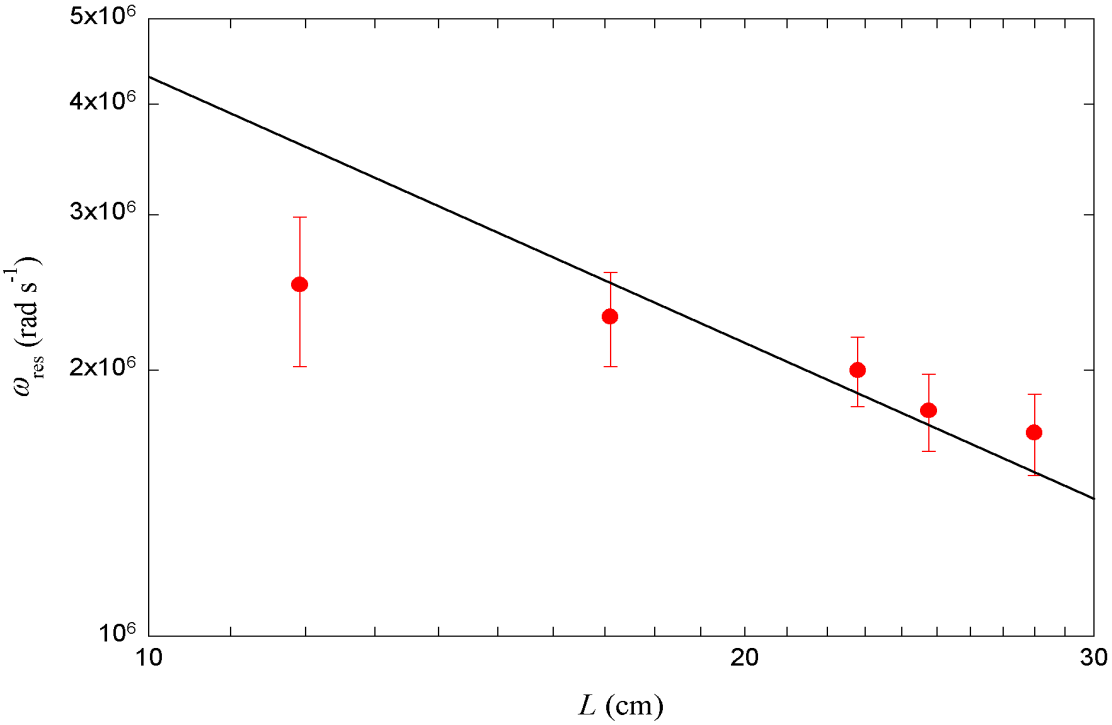

FIGURE 7. The value of ω_{res} decreases as L increases. Excluding the shortest plasma, the data are marginally consistent with a line with slope -1 (solid line).

We find that is difficult to test the radial dependence of the diffusion. Clean measurements are possible only in a small neighborhood near $r \approx 1$ cm. This trouble comes from the noise in the measurements of dn/dr at extreme radii and the measurements of dN/dt at large radii. At large and small radii, $dn/dr \approx 0$ and is therefore susceptible to statistical and numerical noise. At large radii, $dN/dt \approx 0$. In either case, $D \approx (dN/dt)/(dn/dr)$ is poorly behaved.

CONCLUSIONS

We have applied an axially invariant, transverse quadrupole field to a pure electron plasma confined in a Malmberg-Penning trap and observed the effects the quadrupole field has on the shape of the plasma and on transport within the plasma. The quadrupole field distorts the parallel magnetic field lines into flux tubes with elliptical cross sections. Whether the $\boldsymbol{E} \times \boldsymbol{B}$ rotation is faster or slower than the bounce time determines the properties of both the plasma shape and the amount of transport.

If the plasma rotates quickly, we observe the plasma to smear out into a cylinder. If the plasma rotates slowly, we observe that the plasma has the shape of a flux tube, circular in the center and elliptical on each end but with the ellipses rotated by 90° with respect to

one another. The ellipticity is proportional to both the quadrupole field and to the length of the plasma.

The transport created in the plasma by the quadrupole field exhibits a strong resonance in ω. We observe diffusion coefficients of order 1 cm^2/s at resonance for a perturbation of only 0.020 G/cm. This is a weak field compared to those necessary for the confinement of antihydrogen. The field is comparable to what one expects as possible natural quadrupole errors in Malmberg-Penning traps.

By changing the length and temperature of the plasma and observing that the resonant frequency changes accordingly, we have demonstrated that the transport is a bounce resonant effect. The β, ω, B_z and L scalings are consistent with our simple model of the effect, while the kT scaling of our model does not agree with the data. The r dependence proves difficult to test. This disagreements between our model and our experimental observations suggest that perhaps nonresonant particles make a significant contribution to the transport, or perhaps that the transport is not purely diffusive. A model that directly predicts the radial particle flux may better describe our experimental results.

A quadrupole field greatly enhances radial transport in a Malmberg-Penning trap when the plasma is in resonance with the field. Therefore, the ATHENA and ATRAP collaborations will have difficulty using quadrupole fields in conjunction with Malmberg-Penning traps to form antihydrogen. Typical experimental parameters will be $B_z = 2$ T, $n = 10^8$ cm^{-3} and $T = 4$ K [14]. We estimate that $\omega t_b \approx 0.6$, placing them near the resonance. Even if operating off resonance, the magnitude of the quadrupole field will be strong enough to severely limit confinement times.

ACKNOWLEDGMENTS

This work was supported by the Office of Naval Research and by the Los Alamos National Laboratory.

REFERENCES

1. Holzscheiter, M. H., et al., *Hyperfine Interactions*, **109**, 1997 (1997).
2. Gabrielse, G., and S.L. Rolston, L. H., *Phys. Lett. A*, **129**, 38 (1988).
3. Keinigs, R., *Phys. Fluids*, **24**, 1447 (1981).
4. Driscoll, C. F., and Malmberg, J. H., *Phys. Rev. Lett.*, **50**, 167 (1983).
5. Keinigs, R., *Phys. Fluids*, **27**, 206 (1984).
6. Malmberg, J. H., Driscoll, C. F., Beck, B., Eggleston, D. L., Fajans, J., Fine, K., Huang, X. P., and Hyatt, A. W., "Experiments with pure electron plasmas", in *Nonneutral Plasma Physics*, edited by C. Roberson and C. Driscoll, American Institute of Physics, New York, 1988, vol. AIP 175, p. 28.
7. Eggleston, D. L., and O'Neil, T. M., *Phys. Plasmas*, **6**, 2699 (1999).
8. Kriesel, J., and Driscoll, C., *Phys. Rev. Lett.*, **85**, 2510 (2000).
9. Ryutov, D., and Stupakov, G., *Sov. J. Plasma Phys.*, **4**, 278 (1978).
10. Ryutov, D., and Stupakov, G., *Sov. Phys. Dokl.*, **23**, 412 (1978).
11. Cohen, R., *Nuclear Fusion*, **19**, 1579 (1979).
12. Cohen, R., Nevins, W., and Stupakov, G., *Nuclear Fusion*, **23**, 611 (1982).
13. Chirikov, B., *Sov. J. Plasma Phys.*, **5**, 492 (1979).
14. Gabrielse, G. (1999), private communication.